INFECTION AND IMMUNITY, Sept. 2011, p. 3607–3618 Vol. 79, No. 9
0019-9567/11/$12.00 doi:10.1128/IAI.05043-11

Increased Survival and Reduced Neutrophil Infiltration of the Liver in Rab27a- but Not Munc13-4-Deficient Mice in Lipopolysaccharide-Induced Systemic Inflammation▽

Jennifer L. Johnson, Hong Hong, Jlenia Monfregola, and Sergio D. Catz*

Department of Molecular and Experimental Medicine, The Scripps Research Institute, 10550 North Torrey Pines Road, La Jolla, California 92037

Received 10 March 2011/Returned for modification 16 April 2011/Accepted 18 June 2011

Genetic defects in the *Rab27a* or *Munc13-4* gene lead to immunodeficiencies in humans, characterized by frequent viral and bacterial infections. However, the role of Rab27a and Munc13-4 in the regulation of systemic inflammation initiated by Gram-negative bacterium-derived pathogenic molecules is currently unknown. Using a model of lipopolysaccharide-induced systemic inflammation, we show that Rab27a-deficient (Rab27a$^{ash/ash}$) mice are resistant to lipopolysaccharide (LPS)-induced death, while Munc13-4-deficient (Munc13-4$^{jinx/jinx}$) mice show only moderate protection. Rab27a$^{ash/ash}$ but not Munc13-4$^{jinx/jinx}$ mice showed significantly decreased tumor necrosis factor alpha (TNF-α) plasma levels after LPS administration. Neutrophil sequestration in lungs from Rab27a$^{ash/ash}$ and Munc13-4$^{jinx/jinx}$ LPS-treated mice was similar to that observed for wild-type mice. In contrast, Rab27a- but not Munc13-4-deficient mice showed decreased neutrophil infiltration in liver and failed to undergo LPS-induced neutropenia. Decreased liver infiltration in Rab27a$^{ash/ash}$ mice was accompanied by lower CD44 but normal CD11a and CD11b expression in neutrophils. Both Rab27a- and Munc13-4-deficient mice showed decreased azurophilic granule secretion *in vivo*, suggesting that impaired liver infiltration and improved survival in Rab27a$^{ash/ash}$ mice is not fully explained by deficient exocytosis of this granule subset. Altogether, our data indicate that Rab27a but not Munc13-4 plays an important role in neutrophil recruitment to liver and LPS-induced death during endotoxemia, thus highlighting a previously unrecognized role for Rab27a in LPS-mediated systemic inflammation.

The small GTPase Rab27a and its effector Munc13-4 are master regulators of vesicular transport. Genetic defects in the *Rab27a* or *Unc13D* gene lead to immunodeficiency in humans (19, 36). Rab27a deficiency (Griscelli syndrome type 2 [GS2]), an autosomal recessive disorder, is characterized by pigmentary dilution associated with abnormal melanosome transport and immunological defects characterized by impaired cytotoxic T-lymphocyte (CTL), natural killer (NK) cell, and neutrophil functions (29). Munc13-4 deficiency (familial hemophagocytic lymphohistiocytosis 3 [FHL3]) denotes the presence of an underlying genetic disorder in the *Unc13D* gene and presents with an immunologic phenotype similar to that of GS2 but without pigmentation abnormalities, reflecting the more restricted expression of Munc13-4. Patients with Rab27a or Munc13-4 deficiencies develop an accelerated phase of the disease characterized by fever, jaundice, hepatosplenomegaly, pancytopenia, and lymphohistiocytic infiltrates of several organs. The onset of the accelerated phase, known as hemophagocytic lymphohistiocytosis (HLH), is characterized by uncontrolled T-lymphocyte and macrophage activation triggered by viral or bacterial infections (19, 29). Hematological disorders in the Rab27a-deficient (Rab27a$^{ash/ash}$) mouse model of GS2 and the Munc13-4-deficient (Munc13-4$^{jinx/jinx}$) mouse model of FHL3 resemble those present in humans with Griscelli syndrome and Munc13-4 deficiency, respectively (16, 39, 49). This includes malfunction of CTLs, low NK cell activity and, when challenged with appropriate insults, development of HLH (16, 43). Furthermore, in agreement with initial reports describing granulocyte dysfunctions in patients with GS2 (29), previous studies from our laboratory have characterized severe abnormalities in neutrophils from both Rab27a$^{ash/ash}$ and Munc13-4$^{jinx/jinx}$ mice (10, 25, 39).

Neutrophils are the first line of cellular defense of the innate immune system. During microbial infections, neutrophils are exposed to a variety of soluble and particulate stimuli that can differentially modulate the microbicidal capacity of these cells. This includes neutrophil activation by pathogen-associated molecular patterns (PAMPs) through membrane receptors, including Toll-like receptors (TLRs), and by inflammatory cytokines. In particular, TLR4-mediated recognition of the Gram-negative bacterial wall component lipopolysaccharide (LPS) activates several neutrophil functions, including reactive oxygen species production and exocytosis (11). *In vivo* activation of neutrophils by LPS involves expression of adhesion molecules, attachment to the activated endothelium, and migration and release of secretory granule content, including the proinflammatory enzyme myeloperoxidase (MPO). During LPS-induced endotoxemia, neutrophils are sequestered at microcapillaries in several organs, including the lungs and liver (3, 33). Tissue infiltration by neutrophils helps combat disseminated bacterial infections but also frequently results in pro-

* Corresponding author. Mailing address: Department of Molecular and Experimental Medicine, The Scripps Research Institute, 10550 North Torrey Pines Road, La Jolla, CA 92037. Phone: (858) 784-7932. Fax: (858) 784-2054. E-mail: scatz@scripps.edu.

▽ Published ahead of print on 11 July 2011.

tease-mediated tissue damage. Neutrophil functions are dependent on the timely mobilization of secretory organelles to upregulate membrane-associated receptors and adhesion molecules and to release proinflammatory factors that contribute to the amplification of the systemic immune response. Although both Rab27a and Munc13-4 play a central role in the mobilization of secretory organelles in neutrophils (10, 39), the role played by these secretory molecules in the systemic inflammatory response to LPS is currently unknown.

In response to LPS-induced systemic inflammation, neutrophils are sequestered from the blood, a process that is accompanied by tissue and organ infiltration, including that of the lungs and liver (3, 33). The mechanisms mediating neutrophil infiltration appears to be tissue specific. The initial steps in lung infiltration depend on neutrophil expression of lymphocyte function-associated antigen 1 (LFA-1, CD11a/CD18) (3) and β_2 integrin Mac-1 (CD11b/CD18) (38) and by expression of the counterreceptor intercellular adhesion molecule 1 (ICAM-1) in the endothelium of lung capillaries (3, 38) and in the alveolar epithelium (4). Similarly, neutrophil rolling and adhesion in liver postsinusoidal or portal venules requires selectins, β_2 integrins, and endothelial counterreceptors (24). Furthermore neutrophil infiltration and retention in liver sinusoids in response to systemic LPS, where parenchymal cell damage is generally caused by neutrophils (24), is dependent on the interaction of CD44 and hyaluronan, which is postulated to be the dominant mechanism for neutrophil sequestration in liver sinusoids during LPS-induced systemic inflammation (28, 33). This mechanism relies on the expression of the hyaluronan receptor CD44 on the neutrophil plasma membrane (28, 33) and is stimulus specific, as neutrophil infiltration initiated by focal hepatic necrosis is CD11b/CD18 dependent but CD44 independent (34).

Despite the association between bacterial infections and the onset of HLH in FLH-3 and Griscelli syndrome type 2, the close regulation of neutrophil function by lipopolysaccharide, and the role played by Rab27a and Munc13-4 in neutrophil exocytosis, little is known about the function of Rab27a and Munc13-4 in the development and regulation of the systemic inflammatory response to LPS. In this study, we demonstrate that the systemic inflammatory responses of Rab27a- and Munc13-4-deficient mice are strikingly different, and we identify Rab27a as a key player in neutrophil recruitment to liver and LPS-induced lethality during endotoxemia.

MATERIALS AND METHODS

Experimental animal models. Our experiments utilize C57BL/6 *Munc13-4*$^{jinx/jinx}$ mice (referred to here as *jinx* mice) (16), C57BL/6 *Rab27a*$^{ash/ash}$ mice (referred to here as *ashen* mice) (52) and their parental strain, C57BL/6 (wild type [WT]). The Munc13-4-deficient mouse model Munc13-4$^{jinx/jinx}$ was generated by random germ line mutagenesis using the alkylating agent *N*-ethyl-*N*-nitrosourea (16). Based on Western blot analysis, we have previously established that *jinx* mice have a Munc13-4-null phenotype (10). Munc13-4$^{jinx/jinx}$ was maintained as a homozygous stock for use in these studies. *Rab27a*$^{ash/ash}$ mice that contain a splicing mutation in the *Rab27a* gene have been extensively utilized for the study of Rab27a deficiency and were described previously (52). C57BL/6J control mice were obtained from the animal resource center at The Scripps Research Institute. Mice (6 to 8 weeks old) were maintained in a pathogen-free environment and had access to food and water *ad libitum*. All animal studies were performed in compliance with the U.S. Department of Health and Human Services *Guide for the Care and Use of Laboratory Animals* (40). All studies were conducted according to NIH and institutional guidelines and with approval of the animal review board at The Scripps Research Institute.

LPS-induced systemic inflammation. Our experiments utilize *Escherichia coli* LPS of different potencies to yield syndromes and survival rates that evoked different pathogenic stages during endotoxemia. In experiments directed at analyzing cytokine production and neutrophil infiltration into tissues without causing mortality during the study period, sublethal concentrations of LPS were used. In these studies, we used LPS from *E. coli*, serotype R515 (Alexis Biochemicals), a subtype of LPS previously used in similar sublethal *in vivo* studies with C57BL/6 mice (50). For survival assays, we used LPS from *E. coli* 0111:B4 (Calbiochem). This LPS subtype was chosen based on previous studies that found *E. coli* 0111:B4 LPS to induce death with a 90% lethal dose (LD_{90}) in C57BL/6 mice after a single challenge induced by intraperitoneal (i.p.) injection of LPS when used at 8 mg/kg of body weight (41), which largely agrees with the data presented in this work.

For *in vivo* studies of cytokine production and neutrophil infiltration, mice were injected intraperitoneally with a sublethal dose of LPS (4 mg/kg) or vehicle (phosphate-buffered saline [PBS]). LPS (from *E. coli*, serotype R515; Alexis Biochemicals) was diluted in pyrogen-free sterile PBS in a total volume of 500 μl. Blood samples were collected by intraorbital bleeding at 4 and 24 h postinjection. Mice were sacrificed, and tissues were immediately collected, transferred to ice-cold PBS, and processed for myeloperoxidase determination and immunofluorescence analysis. The analyses of tissue and plasma myeloperoxidase were performed using a murine MPO-specific enzyme-linked immunosorbent assay (ELISA; HyCult Biotechnology) according to the manufacturer's instructions. A total of 24 Rab27a$^{ash/ash}$, 20 Munc13-4$^{jinx/jinx}$, and 24 wild-type mice were used in these assays. MPO is an enzyme found in cells of myeloid origin and has been used extensively as a biochemical marker of granulocyte (mainly neutrophil) infiltration into the lung (1) and liver (27). MPO elevation in tissues is due to neutrophil infiltration, as it measures total MPO from all neutrophils in the tissue and is independent of exocytosis. Determination of plasma MPO detects only MPO secreted in response to neutrophil exocytosis but does not measure MPO that remains in neutrophil granules. Plasma levels of tumor necrosis factor alpha (TNF-α) were determined using a singleplex assay specific for murine TNF-α (Invitrogen). For TNF-α secretion assays, a total of 7 mice for each group were analyzed in three independent experiments. Differential leukocyte and platelet counts for Rab27a$^{ash/ash}$, Munc13-4$^{jinx/jinx}$, and control mice were performed using a Hemavet 950 hematology system.

For survival studies, mice were challenged intraperitoneally with 0.5 ml of LPS (7 mg/kg or 12 mg/kg, *E. coli* 0111:B4; Calbiochem). Control mice were injected intraperitoneally with an equal volume of PBS. A total of 12 Rab27a$^{ash/ash}$, 12 Munc13-4$^{jinx/jinx}$, and 18 wild-type mice were used in these assays.

Histology and immunofluorescence analysis. Lungs and livers from LPS- or PBS-treated mice were fixed in Z-Fix (Anatech Ltd., MI) for 24 h and immediately processed with a tissue processor, embedded in paraffin, cut with a microtomer at 3 μm and mounted on slides by following standard procedures. Dewaxing and antigen retrieval were performed exactly as described previously (46). For immunofluorescence staining, samples were incubated in blocking buffer (1% bovine serum albumin [BSA], 0.01% saponin, PBS) for 1 h. The samples were incubated with primary antibodies (diluted 1:200 in blocking buffer) overnight at 4°C, washed with PBS, and labeled with Alexa Fluor-conjugated secondary antibodies. Nuclei were stained with 4′,6′-diamidino-2-phenylindole (DAPI), and samples were preserved in Fluoromount-G mounting medium (SouthernBiotech) and kept at 4°C until analyzed. Samples were analyzed with a Zeiss LSM 710 laser scanning confocal microscope (LSCM) attached to a Zeiss Observer Z1 microscope at 21°C, using a 63× oil Plan Apo, 1.4-numerical-aperture objective. Images were collected using ZEN-LSM software and processed using ImageJ and Adobe Photoshop CS4. The antibodies used for immunofluorescence analysis were anti-mouse MPO (HyCult Biotechnology), anti-mouse Ly-6G (clone A18; BD Pharmingen), anti-ICAM-1 (BD Pharmingen), and anti-P-selectin (BD Pharmingen).

Mice neutrophil isolation. Bone marrow-derived neutrophils were isolated using a Percoll-gradient fractionation system. For neutrophil isolation, a three-layer Percoll gradient was used (52%, 62%, and 78%). Neutrophils were isolated from the 62% to 78% interface, washed, and used in flow cytometry assays. Peripheral murine neutrophils were obtained from blood collected by cardiac puncture, and erythrocytes were removed by lysis using a solution consisting of 168 mM NH_4Cl–10 mM Tris-HCl (pH 7.4). Neutrophils were further isolated using marker-assisted congenic screening (MACS) technology with anti-mouse Ly-6G (clone 1A8) biotin, anti-biotin microbeads, and mass spectrometry (MS) MACS columns, as described by the manufacturer (Miltenyi Biotec).

Flow cytometry analysis. To evaluate the plasma membrane expression of the adhesion molecules CD11b and CD11a in murine neutrophils, blood was ob-

tained by retro-orbital bleeding, and cells were immunostained in whole blood (50 μl) by incubation with the indicated primary antibody or with the isotype control for 30 min at 20°C in the dark. Next, murine erythrocytes were lysed using a hypotonic solution consisting of 168 mM NH_4Cl, 10 mM $KHCO_3$, and 0.097 mM EDTA for 10 min, and leukocytes were fixed with a solution of 1% paraformaldehyde in PBS. Neutrophils were gated based on staining with the granulocyte marker Ly-6G (clone A18). The antibodies used were anti-mouse-CD11b-PE, anti-mouse Ly-6G (clone A18)-fluorescein isothiocyanate (FITC), and anti-mouse CD11a-PE (BD Pharmingen). CD44 expression in bone marrow-derived neutrophils was measured using murine specific anti-CD44-PE monoclonal antibody clone IM7, which specifically recognizes an epitope located between residues 115 and 127 of murine CD44 (37) (BD Pharmingen). The samples were analyzed using a BD FACScan flow cytometer (BD Biosciences) and with FlowJo software.

Adhesion assays. Black, clear-bottom tissue culture polystyrene plates (Corning, Inc.) were coated with fibronectin (Calbiochem) or hyaluronan (5 mg/ml, Acros Organics) in PBS for 12 h at 37°C. The uncoated sites were blocked by treating each well with 200 μl of 0.5% denatured BSA in PBS for 2 h at room temperature (RT). Peripheral neutrophils (3×10^5) were added to each well, and cells were stimulated with 100 ng/ml LPS or 1 μM fMLF or left untreated for 30 min at 37°C. The cells were incubated with Calcein-AM (Anaspec, San Jose, CA) for an additional 30 min, and the percentage of cells that had adhered was estimated by measuring the fluorescence intensity of cells that remained adherent to the coated surfaces following washes with warm (37°C) PBS as described previously (44). All wells were read in duplicate or triplicate using a SpectraMax Gemini EM fluorometer (Molecular Devices). Three independent experiments were performed.

Immunofluorescence and confocal microscopy analysis. For confocal microscopy analysis, BM-derived neutrophils from wild-type or Rab27a$^{ash/ash}$ mice were fixed and permeabilized exactly as described previously (25). The samples were labeled with anti-CD44 (clone IM7; BD Pharmingen) overnight at 4°C and with Alexa Fluor 594-conjugated donkey anti-mouse secondary antibodies (Molecular Probes). The sample were stored in Fluoromount-G (Southern Biotechnology, AL) and analyzed using a Zeiss LSM 710 laser scanning confocal microscope with a 100× oil Plan Apo, 1.4-numerical-aperture objective. Images were processed using ImageJ and Adobe Photoshop CS4.

Statistical analysis. Data are presented as means, and error bars correspond to standard errors of the means (SEM). Statistical significance was determined using the nonparametric Mann-Whitney test unless stated otherwise. Statistical analysis was performed using GraphPad InStat 3, and graphs were made using GraphPad Prism 4. Differences were considered statistically significant at a P value of <0.05.

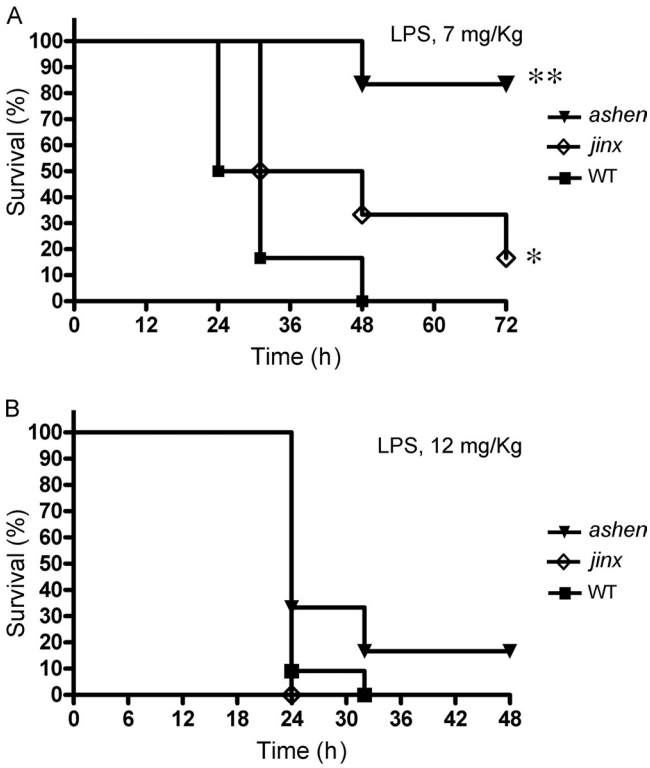

FIG. 1. Kaplan-Meier survival plots for wild-type (WT), Rab27a$^{ash/ash}$ (*ashen*), and Munc13-4 $^{jinx/jinx}$ (*jinx*) mice. Mice were challenged with a single intraperitoneal injection of LPS (7 mg/kg [A] or 12 mg/kg [B]). Survival curves were generated from two independent experiments with a total of 12 Rab27a$^{ash/ash}$, 12 Munc13-4$^{jinx/jinx}$, and 18 wild-type mice. The difference in survival between the wild-type and Rab27a$^{ash/ash}$ mice was significant (**, $P = 0.0012$) by the log-rank test. Although less significant, the difference in survival between wild-type and Munc13-4$^{jinx/jinx}$ mice was also evident (*, $P = 0.05$).

RESULTS

Mice deficient for Rab27a are protected from LPS-induced death. Wild-type (WT), Munc13-4 $^{jinx/jinx}$, and Rab27a$^{ash/ash}$ mice were used in mortality studies. Mice were challenged with a single intraperitoneal injection of 7 mg/kg or 12 mg/kg LPS. In response to 7 mg/kg LPS, 50% of WT mice and 50% of Munc13-4$^{jinx/jinx}$ mice died at 24 h and 32 h, respectively, whereas all Rab27a$^{ash/ash}$ mice were alive at these times (Fig. 1A). All WT mice died within 48 h after challenge; in contrast, 30% of the Munc13-4 $^{jinx/jinx}$ mice and 90% of the Rab27a$^{ash/ash}$ mice were still alive at 48 h. Although most Rab27a$^{ash/ash}$ mice survived and recovered by 72 h, these animals were sick and lethargic after LPS insult. When the higher dose of LPS was used (12 mg/kg), 90% of WT mice and all Munc13-4$^{jinx/jinx}$ mice died by 24 h, while 35% of the Rab27a$^{ash/ash}$ mice survived at this time point (Fig. 1B).

Endotoxemic Rab27a$^{ash/ash}$ mice have low plasma levels of TNF-α. Pro- and anti-inflammatory cytokines play a fundamental role in the development of sepsis in both humans and animal models (6). TNF-α has been strongly associated with septic syndrome (5) and is the prototype of the proinflammatory cytokines leading to activation of multiple cellular responses of the innate immune system during endotoxemia. Furthermore, TNF-α has been shown to modulate CD44 maturation and expression (17) and plays an important role in LPS-induced neutrophil infiltration to the liver (7). Here, we analyzed TNF-α plasma levels in Rab27a$^{ash/ash}$ and Munc13-4$^{jinx/jinx}$ mice after a single insult of lipopolysaccharide. In wild-type mice, TNF-α was detected in plasma 4 h after i.p. LPS injections and returned to basal (undetectable) levels 24 h after LPS challenge (Fig. 2). A sharp increase of TNF-α was also observed with Munc13-4$^{jinx/jinx}$ mice, which showed TNF-α levels that were undistinguishable from those observed with wild-type mice (Fig. 2). In contrast, Rab27a$^{ash/ash}$ mice showed significantly lower TNF-α plasma levels in response to LPS insult, which represent ~50% of the level observed with wild-type mice (Fig. 2). These data strongly support a role for Rab27a in the regulation of TNF-α secretion during LPS-induced systemic inflammation.

Effect of Rab27a and Munc13-4 deficiency on neutrophil sequestration into the lungs during LPS-induced systemic inflammation. Because neutrophil infiltration into the major organs, such as the lung and liver, significantly correlates with the severity of inflammation and is a hallmark of endotoxemia, the effect of LPS treatment on neutrophil infiltration on these tissues was examined. First, we asked whether Rab27a or Munc13-4 plays a significant role in the sequestration of neu-

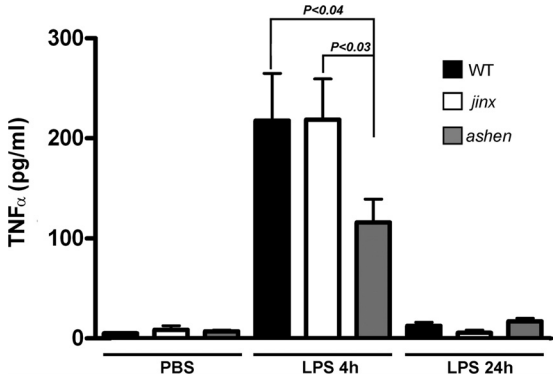

FIG. 2. Mice lacking Rab27a but not Munc13-4 have impaired *in vivo* secretion of TNF-α in response to LPS. Munc13-4$^{jinx/jinx}$ (*jinx*), Rab27a$^{ash/ash}$ (*ashen*), and wild-type (WT) mice were challenged with a single intraperitoneal injection of LPS or PBS. Blood samples were collected at 4 h or 24 h after injection. The samples were spun down, and plasma was collected and analyzed for the presence of TNF-α as described in Materials and Methods. A total of 7 mice for each group were analyzed in three independent experiments. The statistical significance of the difference of the means was calculated using the nonparametric Mann-Whitney test.

trophils to the lungs after LPS insult. To this end, we analyzed neutrophil infiltration by detecting total MPO in lung tissue from LPS-treated mice as described previously (2). We observed a consistent increment of lung-associated MPO in wild-type and Rab27a- and Munc13-4-deficent mice 4 h after LPS insult compared to levels seen with the PBS control (Fig. 3A), although statistically significant differences were reached only in *jinx* mice, a result which most likely is explained by mouse-to-mouse variability in lung-associated MPO levels after LPS treatment. Neutrophil infiltration and permanence in the lungs at 24 h post-LPS insult was previously demonstrated to be dependent on nonendothelial TLR4 (2). Therefore, we next asked whether Rab27a or Munc13-4 could regulate recruitment and residency of neutrophils in lungs specifically at the 24-h time point postinsult. Here, we show that neutrophil sequestration to the lungs also proceeds independently of Rab27a or Munc13-4 expression at 24 h after systemic LPS administration (Fig. 3B). To confirm the results obtained using MPO assays, we analyzed neutrophil sequestration in lungs by immunofluorescence analysis. Infiltrated neutrophils were identified by immunological detection of Ly-6G-positive cells and by nuclear morphology. Neutrophils were identified infiltrating alveolar tissue of wild-type, Munc13-4$^{jinx/jinx}$, and Rab27a$^{ash/ash}$ mice that were treated with LPS but were rarely observed with PBS-treated mice (Fig. 3C). Neutrophils were detected infiltrating alveolar but not bronchial tissue. Next, to rule out a possible defect in endothelium activation in capillaries from Rab27a$^{ash/ash}$ mouse lungs, we evaluated P-selectin expression, which is upregulated in response to LPS stimulation (2). Our results showed marked P-selectin expression in lung capillaries from LPS-treated Rab27a$^{ash/ash}$ mice (Fig. 3D). In these experiments, neutrophils can be detected both adhering to the activated endothelium and transmigrating out of the vasculature (Fig. 3D). Sequestered neutrophils adherent to the endothelium in microcapillaries of lungs from wild-type and Munc13-4$^{jinx/jinx}$ endotoxic mice were also observed (data not shown). Consistent with these observations, we also found that ICAM-1, a molecule constitutively expressed at the surface of alveolar type I epithelial cells (23), which plays a role in the retention and activation of inflammatory cells in the alveoli (14) and in neutrophil recruitment into the lungs during endotoxemia (3), was expressed at similar levels in alveolar epithelium from LPS-treated wild-type, Rab27a$^{ash/ash}$, and Munc13-4$^{jinx/jinx}$ mice (Fig. 3E). Altogether, our data exclude possible defects in the process of neutrophil recruitment to the lungs as the mechanism responsible for the increased survival observed with Rab27a$^{ash/ash}$ mice during LPS-induced endotoxic shock.

Liver sequestration of neutrophils during endotoxemia requires Rab27a but not Munc13-4. Systemic LPS induces neutrophil recruitment to the liver using a mechanism that is different from the classical recruitment model in that neutrophils are sequestered not only in venules but also in sinusoidal capillaries (33). Furthermore, accumulation of neutrophils in the sinusoids may be modulated by both β2 integrin (34) and CD44 (28, 33) expression. Here, we analyzed the effect of Rab27a or Munc13-4 deficiency on neutrophil infiltration into the liver during LPS-induced systemic inflammation. To this end, we first measured liver-associated MPO levels in LPS-treated and untreated mice, a method previously utilized by others to determine neutrophil infiltration in the liver (27). Importantly, although immunohistochemical detection of MPO was previously shown in Kupffer cells (9), this was attributed to MPO from neutrophils engulfed by Kupffer cells (21); therefore, MPO determination is a good parameter of neutrophil infiltration in liver. Furthermore, consistent with previous findings (27), we show that livers from untreated mice have very low levels of MPO (Fig. 4A). Neutrophil-hepatic recruitment was evident in wild-type mice at 4 and 24 h after LPS insult (Fig. 4A and B). Neutrophil infiltration in livers from Rab27a$^{ash/ash}$ and Munc13-4$^{jinx/jinx}$ mice was not significantly different from that observed for wild-type mice when measured 4 h after the intraperitoneal LPS challenge. However, Rab27a$^{ash/ash}$ mice showed a significant decrease in neutrophil sequestration to the liver when measured 24 h after LPS treatment (Fig. 4B). This pattern was observed exclusively with the Rab27a-deficient model, as Munc13-4$^{jinx/jinx}$ mice showed hepatic neutrophil infiltration similar to that observed with wild-type mice, at both 4 h and 24 h (Fig. 4A and B). In agreement with results of tissue-associated MPO assays, immunofluorescence analysis of tissue sections showed the presence of neutrophils adherent to large blood vessels in livers from mice that have been treated with LPS for 4 h (Fig. 4C) but not in those treated with PBS (Fig. 4E). The results suggest that adhesion of neutrophils to portal venules is independent of Munc13-4 and Rab27a. These neutrophils are most likely accountable for the increased levels of liver-associated MPO detected in tissue homogenates at 4 h. Immunofluorescence analysis of livers obtained at 24 h after LPS treatment showed significant neutrophil infiltration in liver sinusoids from both wild-type and Munc13-4$^{jinx/jinx}$ mice (Fig. 4D). In contrast, liver from Rab27a$^{ash/ash}$ mice showed significantly less neutrophil infiltration in response to LPS insult (Fig. 4D), further supporting our observations from tissue MPO detection (Fig. 4B). Altogether, our data suggest that neutrophil retention in liver sinusoids during the LPS-induced systemic inflammatory re-

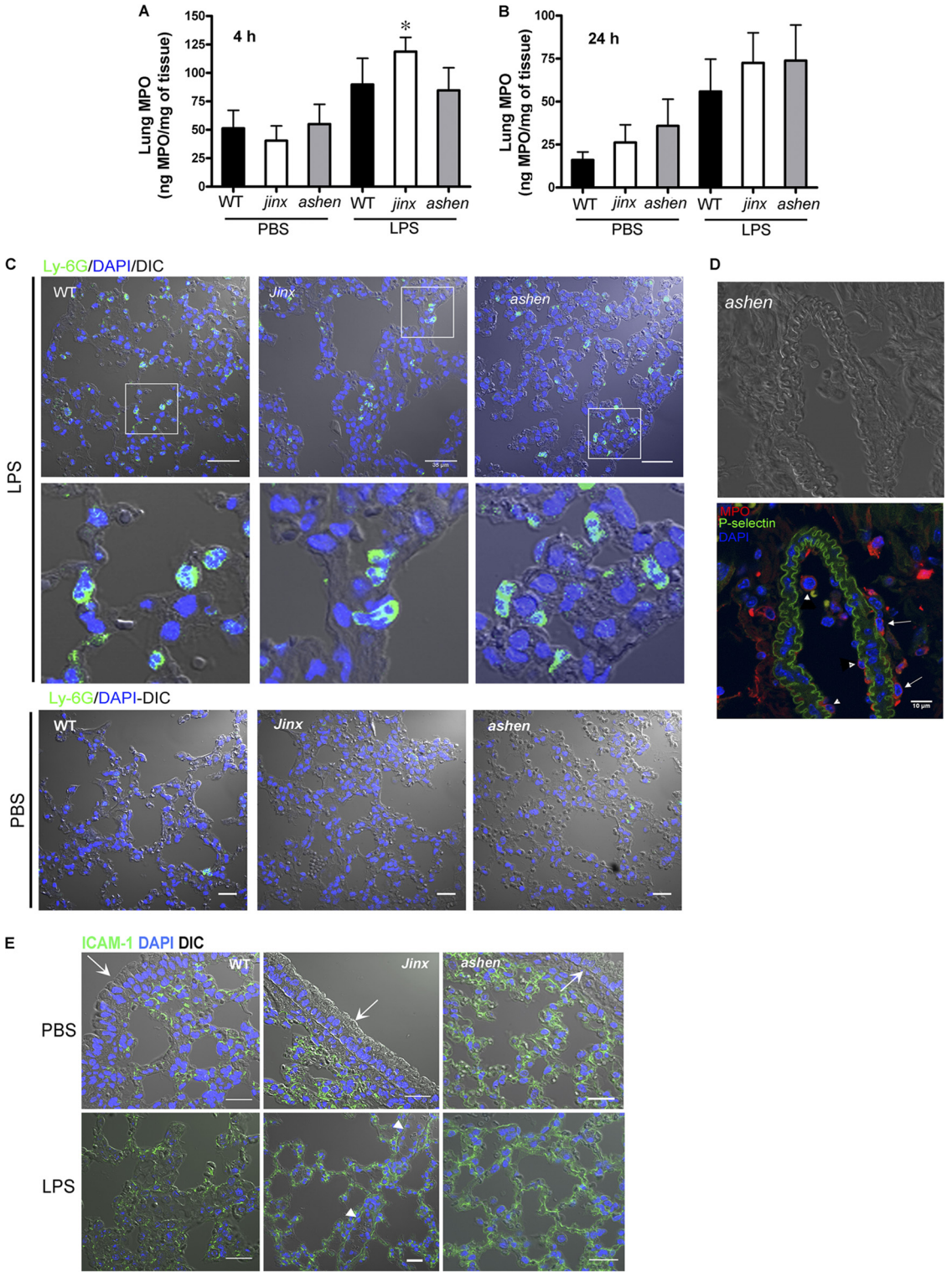

FIG. 3. Rab27a and Munc13-4 are not necessary for neutrophil infiltration into the lungs during LPS-induced systemic inflammation. Neutrophil infiltration into lungs was determined by analysis of tissue-associated myeloperoxidase at 4 h (A) and 24 h (B) after intraperitoneal LPS or PBS injections. Results represent the means ± SEM (n = 5 to 7 mice per group; three independent experiments). *, $P < 0.01$ versus PBS (nonparametric Mann-Whitney test). (C) Representative images of immunofluorescence analysis of Ly-6G-positive cells showing neutrophil infiltration into lungs of wild-type (WT), Rab27a$^{ash/ash}$ (*ashen*), and Munc13-4$^{jinx/jinx}$ (*jinx*) mice 4 h after LPS but not PBS administration. (D) Immunofluorescence analysis showing P-selectin expression in alveolar capillaries from Rab27a$^{ash/ash}$ mice after LPS treatment. Neutrophils, visualized by staining of endogenous MPO (red), are observed both attached to the activated endothelium (arrowheads) and after transendothelial migration (arrows). (E) Immunofluorescence analysis shows expression of ICAM-1 in alveolar walls. Specific staining is also observed in the capillary endothelium (arrowheads) but not in the bronchial epithelium (arrows). Scale bars, 35 μm (C and E), 10 μm (D).

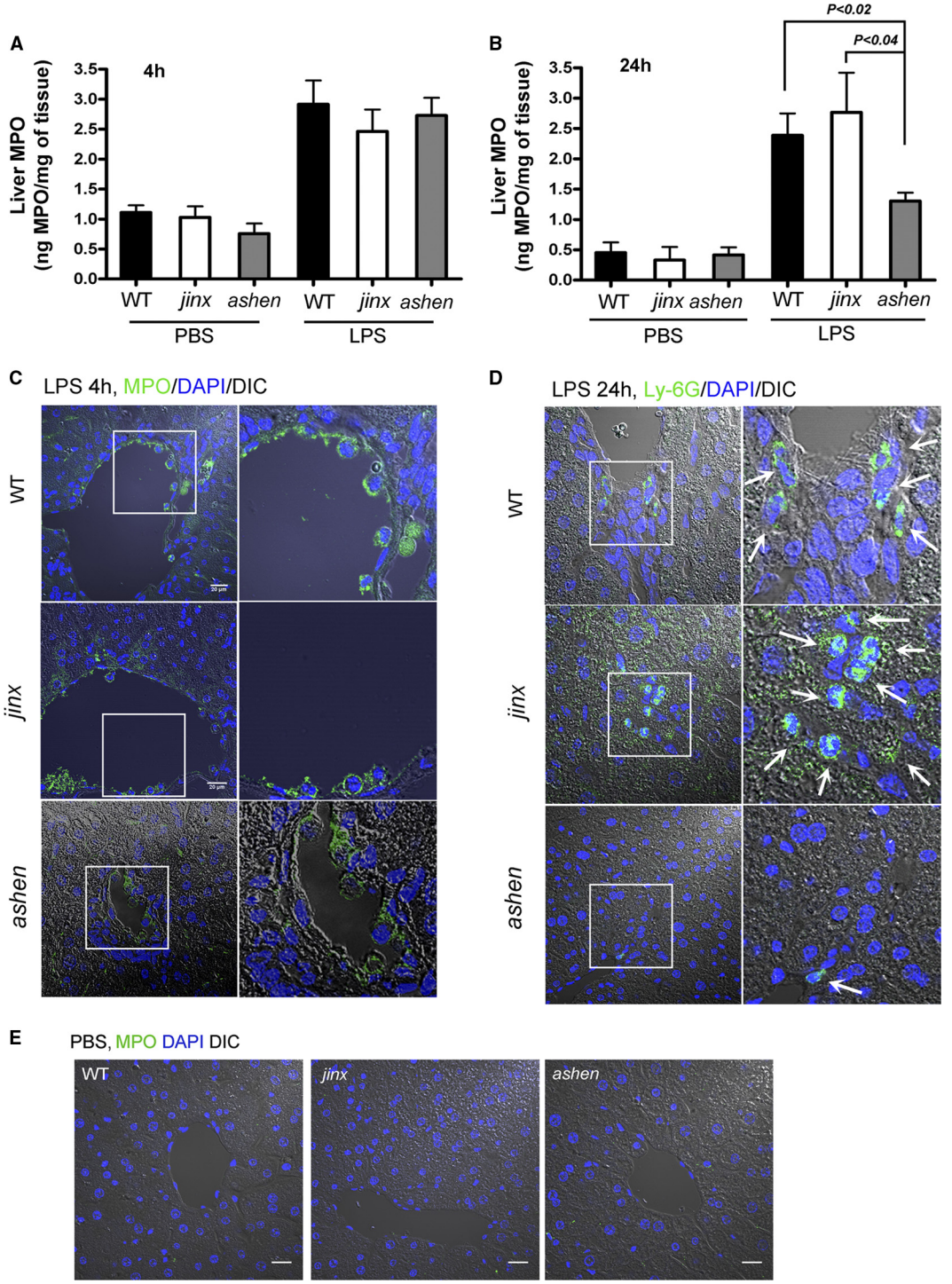

FIG. 4. Liver sequestration of neutrophils during LPS-induced systemic inflammation requires Rab27a but not Munc13-4. Mice were injected intraperitoneally with LPS or PBS, and neutrophil infiltration into the liver was determined by analysis of tissue-associated myeloperoxidase at 4 h (A) and 24 h (B) after injections. Results are presented as means ± SEM. A total of 5 to 7 wild-type and *ashen* mice and 4 *jinx* mice for each condition were analyzed in three independent experiments. The statistical significance of the difference of the means was calculated using the nonparametric Mann-Whitney test. (C) Immunofluorescence analysis of neutrophil infiltration in liver at 4 h postinjection. Representative liver images from LPS-treated mice are shown. (D) Immunofluorescence analysis of neutrophil infiltration at 24 h postinjection of LPS. Infiltrated neutrophils (Ly-6G) are indicated with arrows. (E) Representative liver images from PBS-treated mice. Scale bars, 20 μm (C), 25 μm (E).

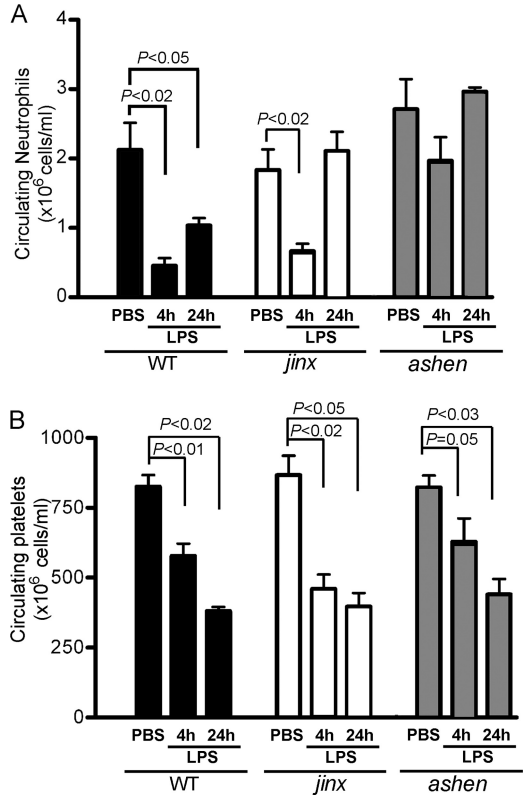

FIG. 5. Effect of systemic LPS on circulating neutrophil and platelet counts in wild-type, Rab27a$^{ash/ash}$, and Munc13-4$^{jinx/jinx}$ mice. Mice were treated with LPS systemically (i.p.) for 4 or 24 h. The numbers of circulating neutrophils (A) and platelets (B) were measured as described in Materials and Methods. The results are presented as means ± SEM. The statistical significance of the difference of the means was calculated using the nonparametric Mann-Whitney test (n = 3 to 6).

sponse is a Rab27a-dependent but Munc13-4-independent mechanism.

Mice deficient in Rab27a or Munc13-4 have different neutrophil responses to LPS *in vivo*. Intraperitoneal administration of LPS in mice and rats induces a rapid inflammatory response characterized by neutrophil sequestration with a consequent marked reduction in circulating neutrophils (2, 15). Neutropenia is induced by systemic inflammation and not by local administration of LPS, which instead evokes neutrophilia (51). To analyze whether decreased liver infiltration correlates with reduced manifestation of neutropenia in endotoxemic mice, we quantified the number of circulating neutrophils in Rab27a$^{ash/ash}$, Munc13-4$^{jinx/jinx}$, and wild-type mice after a single intraperitoneal administration of LPS. The basal number of circulating neutrophils in Rab27a$^{ash/ash}$ and Munc13-4$^{jinx/jinx}$ mice was not significantly different from that observed with unchallenged wild-type mice (Fig. 5A). In response to LPS, wild-type mice showed a marked decrease in the level of circulating neutrophils at 4 h and 24 h after intraperitoneal injections (Fig. 5A). A similar reduction in the number of circulating neutrophils was observed for Munc13-4-deficient mice in response to LPS at 4 h postinjections, although neutrophil counts returned to normal values at 24 h (Fig. 5A). In contrast, Rab27a-deficient mice were not neutropenic at either 4 or 24 h after LPS challenge (Fig. 5A), confirming that neutrophil recruitment in response to LPS-induced systemic inflammation is impaired in Rab27a-deficient mice. This phenotype cannot be explained solely by the observed reduced liver infiltration in Rab27a$^{ash/ash}$ mice in response to LPS, since no defects in neutrophil hepatic infiltration were detected in the Rab27a-deficient model at early time points, suggesting that other organs may also be affected. In contrast to the observed differences in circulating neutrophils, no differences in LPS-induced thrombocytopenia were observed for wild-type, Rab27a$^{ash/ash}$, or Munc13-4$^{jinx/jinx}$ mice (Fig. 5B), suggesting that the defects in neutrophil dynamics observed for Rab27a$^{ash/ash}$ mice cannot be explained by intrinsic abnormalities of the signaling pathway initiated by TLR4 activation.

Role of Rab27a and Munc13-4 in the expression of adhesion molecules in neutrophils during endotoxemia. A role for the β2 integrin subunit CD11b and its counterreceptor ICAM-1 in the sequestration of neutrophils in the endotoxemic liver has been suggested (24). To analyze whether decreased neutrophil recruitment to the liver could be explained by impaired β2 integrin expression in Rab27a$^{ash/ash}$ mice, we first measured CD11b expression in peripheral murine neutrophils obtained after LPS injections. Systemic LPS triggered a significant upregulation of CD11b plasma membrane expression in wild-type neutrophils (Fig. 6A). A similar upregulation of CD11b expression was observed for neutrophils from Rab27a$^{ash/ash}$ and Munc13-4$^{jinx/jinx}$ mice in response to intraperitoneal administration of LPS (Fig. 6A), and no significant differences in the expression of CD11b were detected between neutrophils from the three colonies under study (Fig. 6A). This is in agreement with the observation that adhesion of neutrophils to portal venules, a mechanism proposed to be mediated by β_2 integrins (24), is independent of Munc13-4 and Rab27a (Fig. 4C). Similarly, CD11a, an adhesion molecule that is constitutively expressed in the neutrophil plasma membrane and believed not to be stored in the same granules as CD11b (30), was not significantly upregulated in wild-type, Munc13-4$^{jinx/jinx}$, or Rab27a$^{ash/ash}$ mice in response to LPS treatment *in vivo* (Fig. 6B). In fact, a slight decrease in CD11a expression was observed only for Munc13-4$^{jinx/jinx}$ mice after LPS administration, although the difference did not reach statistical significance (Fig. 6B).

We next asked whether adhesion mechanisms that are dependent on $\alpha_4\beta_1$ and $\alpha_5\beta_1$ integrins, which mediate β_2 integrin-independent leukocyte recruitment during endotoxin-induced inflammation in the lungs (12) and liver (31), could be affected in Rab27a- or Munc13-4-deficient neutrophils. To analyze this, we measured neutrophil adhesion to fibronectin, a process mediated by $\alpha_4\beta_1$ and $\alpha_5\beta_1$ integrins but not β_2 integrins (45). Our data show that neutrophils that do not express Rab27a or Munc13-4 are able to adhere to fibronectin as efficiently as wild-type neutrophils (Fig. 6C), further supporting a lack of Rab27a or Munc13-4 involvement in integrin expression or integrin-dependent adhesion. Furthermore, similar to wild-type neutrophils, Rab27a$^{ash/ash}$ neutrophils showed increased binding to fibronectin when activated with LPS or with the chemotactic peptide fMLF (Fig. 6D). Altogether, our data argue against defects in the expression of β_1 or β_2 integrins in Rab27a-deficient neutrophils.

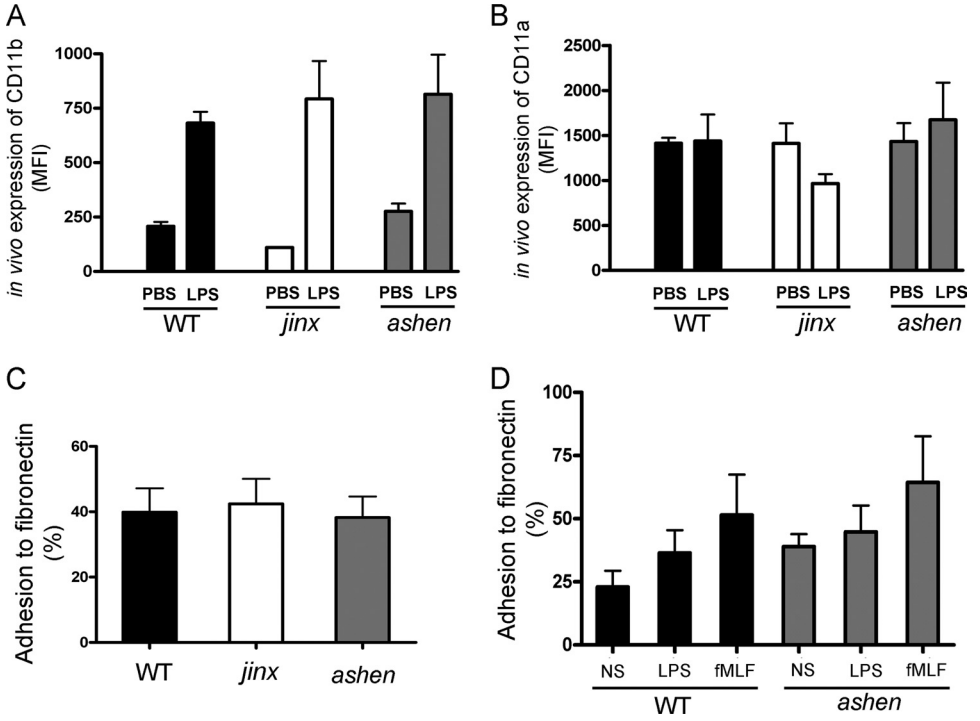

FIG. 6. Effect of systemic LPS on the *in vivo* expression of adhesion molecules in neutrophils from wild-type, Rab27a$^{ash/ash}$, and Munc13-4$^{jinx/jinx}$ mice. (A and B) Mice were injected intraperitoneally with LPS, and blood was collected 4 h after injections. The surface expression of CD11b and CD11a in wild-type (WT), Rab27a$^{ash/ash}$ (*ashen*), and Munc13-4$^{jinx/jinx}$ (*jinx*) neutrophils was analyzed by flow cytometry as described in Materials and Methods. Mean fluorescence intensity (MFI) is shown. (C and D) The adhesion of wild-type (WT), Rab27a$^{ash/ash}$ (*ashen*), and Munc13-4$^{jinx/jinx}$ (*jinx*) neutrophils to fibronectin was measured *ex vivo* as described in Materials and Methods. (A to D) The results are expressed as means ± SEM (n = 3 to 6 mice, three independent experiments).

Neutrophils deficient in Rab27a protein have decreased CD44 surface expression. The adhesion molecule CD44 plays an essential role in neutrophil recruitment to the liver during endotoxemia through its interaction with hyaluronan (33). Here, to test whether a differential expression of CD44 could help explain the decreased hepatic neutrophil recruitment observed with Rab27a$^{ash/ash}$ mice, we analyzed CD44 expression levels in neutrophils by flow cytometry. In Fig. 7A, we show that CD44 expression is significantly decreased in Rab27a$^{ash/ash}$ neutrophils but not in Munc13-4$^{jinx/jinx}$ neutrophils (left panel). Different from that observed for β_2 integrins (26), the plasma membrane expression of CD44 was not significantly upregulated by LPS treatment in wild-type, Rab27a$^{ash/ash}$, or Munc13-4$^{jinx/jinx}$ neutrophils (Fig. 7A, right panel). In fact, a consistent tendency to lower CD44 expression was observed after LPS stimulation, although the differences did not reach statistical significance. To clarify the association between Rab27a and CD44, we analyzed the binding of Rab27a-deficient neutrophils to hyaluronan and performed confocal microscopy studies of the distribution of endogenous CD44 in wild-type and *ashen* mice. The data presented in Fig. 7B show that Rab27a-deficient neutrophils have an impaired mechanism of binding to hyaluronan that links the significantly lower level of CD44 expression with the lower level of neutrophil liver infiltration in *ashen* mice. The confocal microscopy analysis presented in Fig. 7C shows that the distribution of CD44 in *ashen* mouse neutrophils is not different from that in wild-type mice. However, while stimulated wild-type mouse neutrophils showed the characteristic elongated shape after treatment with the chemotactic peptide fMLF, resulting in more dispersed distribution of CD44 at the plasma membrane, this phenotype was less evident in *ashen* mouse neutrophils, suggesting that CD44 presentation may be impaired in the absence of Rab27a (Fig. 7C, lower panels).

Both Rab27a- and Munc13-4-deficient mice have impaired *in vivo* secretion of MPO. Myeloperoxidase-null (MPO$^{-/-}$) mice are characterized by reduced sepsis-induced lung injury and mortality (8). Rab27a and Munc13-4 are thought to be components of a common secretory machinery in a variety of cells types, and in neutrophils, they regulate MPO secretion by controlling the exocytosis of azurophilic granules (10, 39). Since both MPO$^{-/-}$ and Rab27a$^{ash/ash}$ but not Munc13-4$^{jinx/jinx}$ mice show increased survival to LPS insult, we asked whether decreased MPO secretion was associated with this phenotype. To this end, we analyzed whether Rab27a and Munc13-4 play a significant role in MPO secretion in response to systemic LPS treatment. The results presented here show a marked increase in MPO plasma concentration in wild-type mice and significantly lower levels of MPO in plasma from Rab27a$^{ash/ash}$ mice after LPS challenge (Fig. 8A). These data confirm previous results obtained using a different mouse model of Rab27a deficiency (39) and support a role for Rab27a in LPS-induced MPO exocytosis. Next, we reason that if decreased death could be explained only by reduced MPO secretion, Munc13-4-deficient mice, which are more susceptible to LPS-induced death than Rab27a-deficient mice, should show a milder defect in

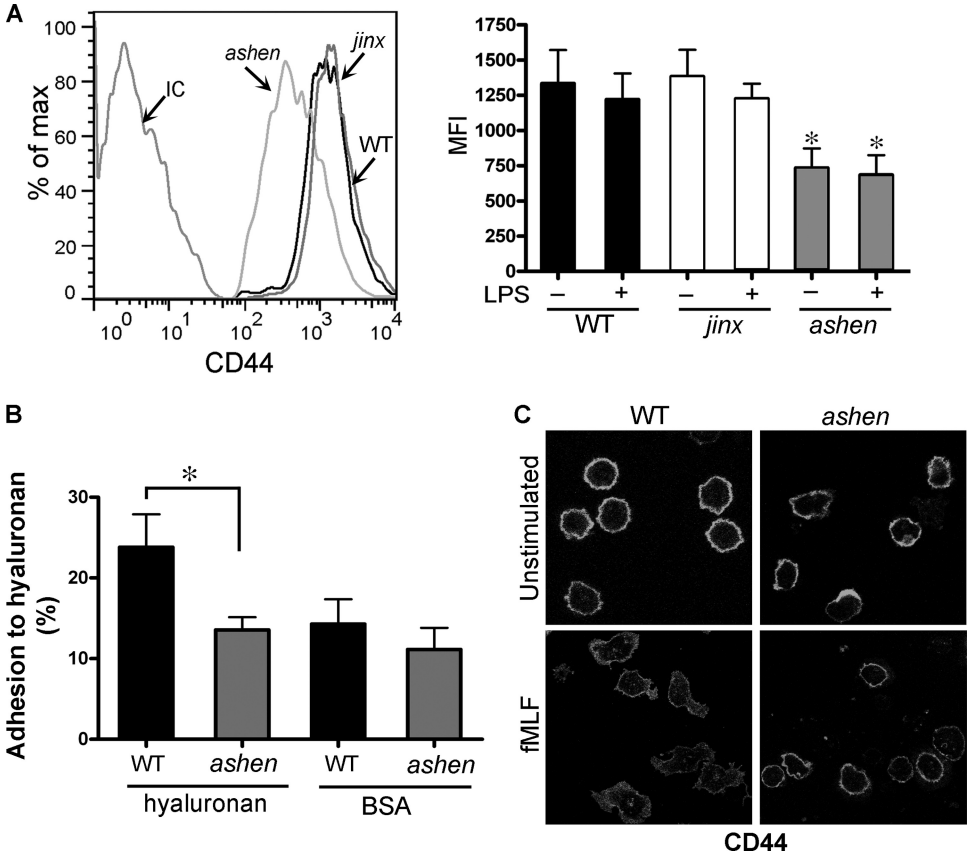

FIG. 7. Rab27a-deficient neutrophils have decreased CD44 surface expression. (A) The surface expression of the hyaluronan receptor CD44 in neutrophils was analyzed by flow cytometry. Left panel, representative histograms of CD44 expression in unstimulated neutrophils from Rab27a$^{ash/ash}$ (*ashen*), Munc13-4$^{jinx/jinx}$ (*jinx*), or wild-type (WT) mice after labeling with a monoclonal antibody directed at an extracellular epitope of CD44 (clone IM7) or isotype control (IC). Right panel, quantitative analysis of the MFI corresponding to CD44 expression in LPS-stimulated (100 ng/ml) and unstimulated neutrophils. Results are represented as means ± SEM ($n = 6$ mice). ∗, $P < 0.03$ versus the wild-type mice. (B) The adhesion of wild-type (WT) and Rab27a$^{ash/ash}$ (*ashen*) bone marrow-derived neutrophils to hyaluronan was measured *ex vivo* as described in Materials and Methods. Results are means ± SEM from three independent experiments using cells from 3 wild-type and 4 *ashen* mice. ∗, $P < 0.03$ (nonparametric Mann-Whitney test). (C) Immunofluorescence analysis of the distribution of endogenous CD44 in *ashen* and wild-type neutrophils, unstimulated or treated with the chemotactic peptide fMLF. Data are representative of results of two independent experiments.

MPO secretion. In Fig. 8B, we show that Munc13-4$^{jinx/jinx}$ mice have impaired MPO secretion in response to systemic LPS challenge, similar to that observed for Rab27a$^{ash/ash}$ mice. Importantly, no significant differences were observed in total MPO expression between unstimulated control, Rab27a$^{ash/ash}$, and Munc13-4$^{jinx/jinx}$ neutrophils (26), suggesting that the differences in plasma MPO levels observed after intraperitoneal administration of LPS are intrinsic to a defect in azurophilic granule exocytosis. Altogether, our results suggest that increased survival in endotoxemic Rab27a$^{ash/ash}$ mice cannot be fully explained by decreased myeloperoxidase release. Importantly, neutrophils are able to secrete only 20% of their total cellular MPO even at maximum stimulation (48). This is explained by the observation that only 20% of total azurophilic granules in a given neutrophil possess the necessary secretory proteins to engage in exocytosis (39). Thus, it is expected that during endotoxemia, circulating wild-type neutrophils lose a maximum of 20% of their total MPO, while Rab27a-deficient neutrophils will most likely conserve this extra 20%. Therefore, the decrease in neutrophil infiltration into the liver observed for Rab27a-deficient mice, measured by analysis of total liver MPO, is probably an underestimation due to the maximum 20% loss of MPO in wild-type neutrophils. These data validate the use of MPO as a marker of neutrophil infiltration despite the role played by Rab27a in MPO exocytosis and further support the observation that neutrophil infiltration into the liver is deficient in *ashen* mice.

DISCUSSION

Rab27a and Munc13-4 play important roles in the regulation of inflammatory cell functions and immunity, and their deficiencies are associated with immunodeficiencies in humans and mice. In this study, we show that Rab27a deficiency is associated with increased survival and reduced neutrophil infiltration of the liver in a model of LPS-induced systemic inflammation. The role of Rab27a in LPS-induced systemic inflammation is regulated at many levels: first, mice that lack Rab27a expression have significantly decreased TNF-α secretion in response to LPS. Second, at the neutrophil level, membrane expression of the adhesion molecule CD44, which mediates sequestration of neutrophils in liver sinusoids, is de-

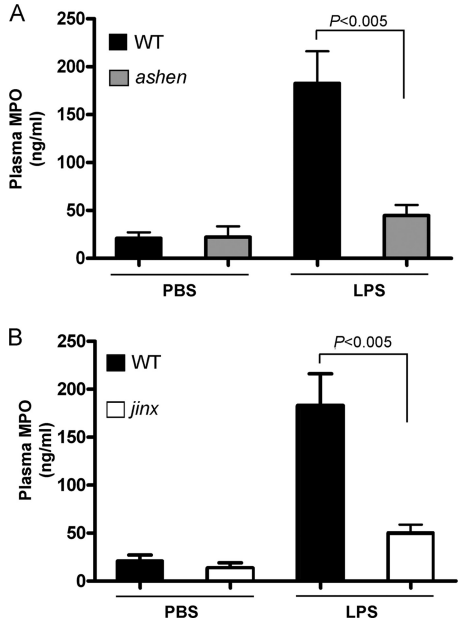

FIG. 8. Mice lacking Rab27a or Munc13-4 have impaired *in vivo* secretion of MPO in response to LPS. Rab27a$^{ash/ash}$ (*ashen*) (A) or Munc13-4$^{jinx/jinx}$ (*jinx*) (B) and wild-type (WT) mice were challenged with a single intraperitoneal injection of LPS or PBS. Blood samples were collected at 4 h after injection. The samples were spun down, and plasma was collected and analyzed for the presence of MPO using a mouse-specific ELISA. The statistical significance of the difference of the means was calculated using the nonparametric Mann-Whitney test ($n = 6$ mice, three independent experiments).

creased in the absence of Rab27a expression. Third, decreased myeloperoxidase in plasma from Rab27a-deficient mice may also contribute, at least in part, to the increased survival of these mice to LPS challenge. In contrast to results observed with the Rab27a-deficient model, mice deficient in the expression of the effector molecule Munc13-4 conserved their ability to secrete TNF-α, expressed the hyaluronan receptor CD44 in neutrophils, and showed normal neutrophil recruitment into liver and lungs. Although Munc13-4-deficient mice showed impaired *in vivo* MPO secretion, they had only moderate resistance to LPS-induced death. Altogether, our results provide insight into the mechanisms regulated by Rab27a in LPS-induced systemic inflammation and suggest that this small GTPase plays a central role in the regulation of LPS-induced neutrophil infiltration to the liver and death.

During LPS-induced liver injury, TNF-α facilitates the extravasation of neutrophils into the liver parenchyma, which produces cytotoxic liver cell damage (7, 47). Importantly, passive immunization against TNF-α protects mice from the lethal effects of endotoxin, and TNF-α alone can induce some of the deleterious effects of LPS (5). Our observations that Rab27a$^{ash/ash}$ but not Munc13-4$^{jinx/jinx}$ mice have decreased plasma levels of TNF-α after LPS administration suggests that Rab27a controls the process of regulated secretion of this cytokine during endotoxemia through Rab27a-effectors different from Munc13-4. Although TNF-α is produced by macrophages, Kupffer cells, and to a lesser extent by neutrophils (13), only mast cells are able to store the active cytokine in readily releasable secretory granules and secrete TNF-α through the regulated secretory pathway (20). Furthermore, mast cells were proposed to provide the only readily available source of TNF-α within peripheral tissues during the early course of infection (35). Our results showing that Rab27a, a master controller of regulated secretion, is necessary for maintaining TNF-α levels during the course of inflammation, suggest that Rab27a may be a key regulator of TNF-α secretion from mast cells. However, a possible role for Rab27a in the regulation of TNF-α secretion and production of other inflammatory mediators by macrophages, which are involved in neutrophil infiltration into the liver during endotoxemia, cannot be ruled out at this time. To address this issue, future efforts in our laboratory will focus on the analysis of TNF-α secretion as well as chemokine production by Rab27a-deficient liver macrophages during endotoxemia.

Neutrophil infiltration is one of the major factors responsible for hepatic toxicity during systemic inflammation (24). Recent studies demonstrated that neutrophil sequestration at liver sinusoids is mediated by the interaction of the cell surface adhesion molecule CD44 with the extracellular matrix component hyaluronan and that neutrophil CD44 but not endothelial CD44 is necessary for neutrophil sequestration (33). The mechanism that regulates CD44 expression in neutrophils is currently unknown. In this study, we show that neutrophils that lack Rab27a have lower levels of expression of CD44, which correlates with impaired binding to hyaluronan and decreased neutrophil sequestration in the liver in Rab27a-deficient mice, suggesting that the small GTPase is necessary to maintain relatively elevated levels of CD44 expression at the plasma membrane in neutrophils. At least two mechanisms can possibly explain the role of Rab27a in CD44 expression. First, CD44 may be stored in neutrophil secretory organelles and, in response to stimuli, CD44 would be translocated to the plasma membrane in a Rab27a-dependent manner; second, Rab27a may regulate trafficking of recycling endosomes carrying CD44 toward the plasma membrane. Based on *in vitro* experiments showing lack of upregulation of CD44 surface expression in LPS-treated wild-type cells and on confocal microscopy analysis showing a lack of endogenous CD44 distribution in intracellular structures in unstimulated cells, we speculate that Rab27a regulates a vesicular trafficking mechanism different from secretory organelle exocytosis to mediate CD44 upregulation. Our observation that CD44 distribution at the plasma membrane is characterized by a dispersed pattern in wild-type cells but not in cells that lack Rab27a, suggest that Rab27a may be important in redistribution of CD44 to plasma membrane microdomains to facilitate its presentation.

Apart from its role in the generation of reactive oxygen species, myeloperoxidase has important biological roles during inflammation and infection. In particular, MPO secreted from neutrophils catalytically consumes and limits nitric oxide (NO) availability and contributes to vascular endothelium dysfunction during acute inflammation (18). Supporting this, MPO deficiency is associated with increased NO production and reduced sepsis-induced lung injury (8). Since Rab27a and Munc13-4 regulate azurophilic granule exocytosis in neutrophils, we investigated whether some of the phenotypic characteristics observed with the endotoxemic Rab27a-deficient mice could be explained by a deficiency of *in vivo* MPO secretion. In this study, we show for the first time that Munc13-4-deficient

mice have impaired *in vivo* secretion of MPO. Despite the similar defects in MPO secretion in the two mouse models, increased survival after LPS insult was markedly manifested in Rab27a-deficient mice but only modestly apparent in the Munc13-4-deficient model. Therefore, the protective effect of Rab27a deficiency on LPS-induced death is unlikely to be explained solely by the defect in azurophilic granule exocytosis observed for these mice.

Hemophagocytic lymphohistiocytosis (HLH) is a hallmark of both Rab27a and Munc13-4 deficiencies in humans and presents with nearly identical clinical features in GS2 and FHL patients, leading to death in the absence of therapy (32). Recurrent viral and bacterial infections, including some mediated by Gram-negative bacteria, have been associated with hemophagocytic lymphohistiocytosis in genetically predisposed patients, in which HLH is frequently accompanied by hepatomegaly and neutropenia (32). Furthermore, TNF-α is upregulated in HLH and may contribute to the pathogenesis of hemophagocytic syndrome (22), and recent studies showed that the neutrophil chemoattractant interleukin-8 (IL-8) is upregulated in some patients with FHL (42). Although neutrophils are not considered a first-line problem in HLH, recent evidence suggests that neutrophil recruitment to sites of active disease participate in the deleterious events during the accelerated phase of the disease (42). Our results suggest that there may be previously underappreciated differences between the systemic inflammatory responses triggered by Gram-negative bacterial infections in patients suffering from GS2 and FHL-3 and that differences in TNF-α secretion and neutrophil activation levels may play a significant role in this mechanism. However, it is noteworthy that TNF-α secretion is impaired but not abolished in *ashen* mice and that LPS challenge in the absence of infection is unable to induce HLH in these mice. Future experiments using infectious agents to trigger HLH in *ashen* mice will help elucidate the role of TNF-α and neutrophils in the pathogenesis of HLH.

Altogether, our data support a role for Rab27a in LPS-induced death and neutrophil recruitment to the liver during endotoxemia that is independent of Munc13-4 function. This effect seems to be regulated at many levels, including TNF-α secretion and surface expression of the adhesion molecule CD44 in neutrophils. Our results highlight Rab27a as a potential target for the prevention of neutrophil-mediated inflammatory hepatotoxicity during endotoxemia.

ACKNOWLEDGMENTS

This work was supported by U.S. Public Health Service grant HL088256 to S.D.C.

We are thankful to Bruce Beutler for contributing the Munc13-4-deficient mice and for discussions on LPS-induced inflammation. We thank John Griffin for help with survival assays and Tho Ta for assistance with animal handling and care.

REFERENCES

1. **Andonegui, G., et al.** 2003. Endothelium-derived Toll-like receptor-4 is the key molecule in LPS-induced neutrophil sequestration into lungs. J. Clin. Invest. **111:**1011–1020.
2. **Andonegui, G., et al.** 2009. Mice that exclusively express TLR4 on endothelial cells can efficiently clear a lethal systemic Gram-negative bacterial infection. J. Clin. Invest. **119:**1921–1930.
3. **Basit, A., et al.** 2006. ICAM-1 and LFA-1 play critical roles in LPS-induced neutrophil recruitment into the alveolar space. Am. J. Physiol. Lung Cell. Mol. Physiol. **291:**L200–L207.
4. **Beck-Schimmer, B., et al.** 2002. Role of alveolar epithelial ICAM-1 in lipopolysaccharide-induced lung inflammation. Eur. Respir. J. **19:**1142–1150.
5. **Beutler, B., I. W. Milsark, and A. C. Cerami.** 1985. Passive immunization against cachectin/tumor necrosis factor protects mice from lethal effect of endotoxin. Science **229:**869–871.
6. **Blackwell, T. S., and J. W. Christman.** 1996. Sepsis and cytokines: current status. Br. J. Anaesth. **77:**110–117.
7. **Bradham, C. A., J. Plumpe, M. P. Manns, D. A. Brenner, and C. Trautwein.** 1998. Mechanisms of hepatic toxicity. I. TNF-induced liver injury. Am. J. Physiol. **275:**G387–G392.
8. **Brovkovych, V., et al.** 2008. Augmented inducible nitric oxide synthase expression and increased NO production reduce sepsis-induced lung injury and mortality in myeloperoxidase-null mice. Am. J. Physiol. Lung Cell. Mol. Physiol. **295:**L96–103.
9. **Brown, K. E., E. M. Brunt, and J. W. Heinecke.** 2001. Immunohistochemical detection of myeloperoxidase and its oxidation products in Kupffer cells of human liver. Am. J. Pathol. **159:**2081–2088.
10. **Brzezinska, A. A., et al.** 2008. The Rab27a effectors JFC1/Slp1 and Munc13-4 regulate exocytosis of neutrophil granules. Traffic **9:**2151–2164.
11. **Brzezinska, A. A., J. L. Johnson, D. B. Munafo, B. A. Ellis, and S. D. Catz.** 2009. Signalling mechanisms for Toll-like receptor-activated neutrophil exocytosis: key roles for interleukin-1-receptor-associated kinase-4 and phosphatidylinositol 3-kinase but not Toll/IL-1 receptor (TIR) domain-containing adaptor inducing IFN-beta (TRIF). Immunology **127:**386–397.
12. **Burns, J. A., T. B. Issekutz, H. Yagita, and A. C. Issekutz.** 2001. The alpha 4 beta 1 (very late antigen (VLA)-4, CD49d/CD29) and alpha 5 beta 1 (VLA-5, CD49e/CD29) integrins mediate beta 2 (CD11/CD18) integrin-independent neutrophil recruitment to endotoxin-induced lung inflammation. J. Immunol. **166:**4644–4649.
13. **Cassatella, M. A.** 1995. The production of cytokines by polymorphonuclear neutrophils. Immunol. Today **16:**21–26.
14. **Churchill, L., R. H. Gundel, L. G. Letts, and C. D. Wegner.** 1993. Contribution of specific cell-adhesive glycoproteins to airway and alveolar inflammation and dysfunction. Am. Rev. Respir. Dis. **148:**S83–S87.
15. **Coughlan, A. F., H. Hau, L. C. Dunlop, M. C. Berndt, and W. W. Hancock.** 1994. P-Selectin and platelet-activating factor mediate initial endotoxin-induced neutropenia. J. Exp. Med. **179:**329–334.
16. **Crozat, K., et al.** 2007. Jinx, an MCMV susceptibility phenotype caused by disruption of Unc13d: a mouse model of type 3 familial hemophagocytic lymphohistiocytosis. J. Exp. Med. **204:**853–863.
17. **Delcommenne, M., R. Kannagi, and P. Johnson.** 2002. TNF-alpha increases the carbohydrate sulfation of CD44: induction of 6-sulfo N-acetyl lactosamine on N- and O-linked glycans. Glycobiology **12:**613–622.
18. **Eiserich, J. P., et al.** 2002. Myeloperoxidase, a leukocyte-derived vascular NO oxidase. Science **296:**2391–2394.
19. **Feldmann, J., et al.** 2003. Munc13-4 is essential for cytolytic granules fusion and is mutated in a form of familial hemophagocytic lymphohistiocytosis (FHL3). Cell **115:**461–473.
20. **Gordon, J. R., and S. J. Galli.** 1990. Mast cells as a source of both preformed and immunologically inducible TNF-alpha/cachectin. Nature **346:**274–276.
21. **Gregory, S. H., and E. J. Wing.** 2002. Neutrophil-Kupffer cell interaction: a critical component of host defenses to systemic bacterial infections. J. Leukoc. Biol. **72:**239–248.
22. **Henter, J. I., et al.** 1991. Hypercytokinemia in familial hemophagocytic lymphohistiocytosis. Blood **78:**2918–2922.
23. **Hill, P. A., H. Y. Lan, D. J. Nikolic-Paterson, and R. C. Atkins.** 1994. Pulmonary expression of ICAM-1 and LFA-1 in experimental Goodpasture's syndrome. Am. J. Pathol. **145:**220–227.
24. **Jaeschke, H., and T. Hasegawa.** 2006. Role of neutrophils in acute inflammatory liver injury. Liver Int. **26:**912–919.
25. **Johnson, J. L., et al.** 2010. Rab27a and Rab27b regulate neutrophil azurophilic granule exocytosis and NADPH oxidase activity by independent mechanisms. Traffic **11:**533–547.
26. **Johnson, J. L., H. Hong, J. Monfregola, W. B. Kiosses, and S. D. Catz.** 2011. MUNC13-4 restricts motility of RAB27A-expressing vesicles to facilitate lipopolysaccharide-induced priming of exocytosis in neutrophils. J. Biol. Chem. **286:**5647–5656.
27. **Kato, A., C. Gabay, T. Okaya, and A. B. Lentsch.** 2002. Specific role of interleukin-1 in hepatic neutrophil recruitment after ischemia/reperfusion. Am. J. Pathol. **161:**1797–1803.
28. **Khan, A. I., et al.** 2004. Role of CD44 and hyaluronan in neutrophil recruitment. J. Immunol. **173:**7594–7601.
29. **Klein, C., et al.** 1994. Partial albinism with immunodeficiency (Griscelli syndrome). J. Pediatr. **125:**886–895.
30. **Kuijpers, T. W., et al.** 1991. Membrane surface antigen expression on neutrophils: a reappraisal of the use of surface markers for neutrophil activation. Blood **78:**1105–1111.
31. **Lee, W. Y., and P. Kubes.** 2008. Leukocyte adhesion in the liver: distinct adhesion paradigm from other organs. J. Hepatol. **48:**504–512.
32. **Mahlaoui, N., et al.** 2007. Immunotherapy of familial hemophagocytic lymphohistiocytosis with antithymocyte globulins: a single-center retrospective report of 38 patients. Pediatrics **120:**e622–e628.

33. **McDonald, B., et al.** 2008. Interaction of CD44 and hyaluronan is the dominant mechanism for neutrophil sequestration in inflamed liver sinusoids. J. Exp. Med. **205:**915–927.
34. **McDonald, B., et al.** 2010. Intravascular danger signals guide neutrophils to sites of sterile inflammation. Science **330:**362–366.
35. **McLachlan, J. B., et al.** 2003. Mast cell-derived tumor necrosis factor induces hypertrophy of draining lymph nodes during infection. Nat. Immunol. **4:**1199–1205.
36. **Menasche, G., et al.** 2000. Mutations in RAB27A cause Griscelli syndrome associated with haemophagocytic syndrome. Nat. Genet. **25:**173–176.
37. **Mikecz, K., F. R. Brennan, J. H. Kim, and T. T. Glant.** 1995. Anti-CD44 treatment abrogates tissue oedema and leukocyte infiltration in murine arthritis. Nat. Med. **1:**558–563.
38. **Moreland, J. G., R. M. Fuhrman, J. A. Pruessner, and D. A. Schwartz.** 2002. CD11b and intercellular adhesion molecule-1 are involved in pulmonary neutrophil recruitment in lipopolysaccharide-induced airway disease. Am. J. Respir. Cell Mol. Biol. **27:**474–480.
39. **Munafo, D. B., et al.** 2007. Rab27a is a key component of the secretory machinery of azurophilic granules in granulocytes. Biochem. J. **402:**229–239.
40. **National Research Council.** 1996. Guide for the care and use of laboratory animals. National Academy Press, Washington, DC.
41. **Niessen, F., et al.** 2008. Dendritic cell PAR1-S1P3 signalling couples coagulation and inflammation. Nature **452:**654–658.
42. **Nold-Petry, C. A., et al.** 2010. Failure of interferon gamma to induce the anti-inflammatory interleukin 18 binding protein in familial hemophagocytosis. PLoS One **5:**e8663.
43. **Pachlopnik Schmid, J., et al.** 2009. Neutralization of IFNgamma defeats haemophagocytosis in LCMV-infected perforin- and Rab27a-deficient mice. EMBO Mol. Med. **1:**112–124.
44. **Pereira, S., and C. Lowell.** 2003. The Lyn tyrosine kinase negatively regulates neutrophil integrin signaling. J. Immunol. **171:**1319–1327.
45. **Reinhardt, P. H., J. F. Elliott, and P. Kubes.** 1997. Neutrophils can adhere via alpha4beta1-integrin under flow conditions. Blood **89:**3837–3846.
46. **Robertson, D., K. Savage, J. S. Reis-Filho, and C. M. Isacke.** 2008. Multiple immunofluorescence labelling of formalin-fixed paraffin-embedded (FFPE) tissue. BMC Cell Biol. **9:**13.
47. **Schlayer, H. J., et al.** 1988. Involvement of tumor necrosis factor in endotoxin-triggered neutrophil adherence to sinusoidal endothelial cells of mouse liver and its modulation in acute phase. J. Hepatol. **7:**239–249.
48. **Sengelov, H., L. Kjeldsen, and N. Borregaard.** 1993. Control of exocytosis in early neutrophil activation. J. Immunol. **150:**1535–1543.
49. **Stinchcombe, J. C., et al.** 2001. Rab27a is required for regulated secretion in cytotoxic T lymphocytes. J. Cell Biol. **152:**825–834.
50. **Sutton, C., C. Brereton, B. Keogh, K. H. Mills, and E. C. Lavelle.** 2006. A crucial role for interleukin (IL)-1 in the induction of IL-17-producing T cells that mediate autoimmune encephalomyelitis. J. Exp. Med. **203:**1685–1691.
51. **Vandal, K., et al.** 2003. Blockade of S100A8 and S100A9 suppresses neutrophil migration in response to lipopolysaccharide. J. Immunol. **171:**2602–2609.
52. **Wilson, S. M., et al.** 2000. A mutation in Rab27a causes the vesicle transport defects observed in ashen mice. Proc. Natl. Acad. Sci. U. S. A. **97:**7933–7938.

Editor: S. R. Blanke